ONLINE FIRST



**ISSN:** 0015-5659

**e-ISSN:** 1644-3284

# Synergistic effect of curcumin and adriamycin on apoptosis in retinal tumor cells: a molecular and cellular analysis

**Authors**: Semih Doğan, Mehmet Cudi Tuncer, İlhan Özdemir

**DOI:** 10.5603/fm.104970

**Article type:** Original article

**Submitted:** 2025-02-17

**Accepted:** 2025-03-05

**Published online:** 2025-03-21

ORIGINAL ARTICLE

# Synergistic effect of curcumin and adriamycin on apoptosis in retinal tumor cells: a molecular and cellular analysis

Semih Doğan[1] https://orcid.org/0000-0002-9348-3990, Mehmet Cudi Tuncer[2] https://orcid.org/0000-0001-7317-5467, İlhan Özdemir[3] https://orcid.org/0000-0001-9957-0211

[1]Department of Ophthalmology, Faculty of Medicine, Beykent University, Istanbul, Turkey

[2]Department of Anatomy, Faculty of Medicine, Dicle University, Diyarbakır, Turkey

[3]Department of Gynecology and Obstetrics, Faculty of Medicine, Atatürk University, Erzurum, Turkey

Address for correspondende: Prof. M. Cudi Tuncer, Dicle University, Medical School, Chief of Anatomy Department, Diyarbakır, Turkey; tel. +90 412 2488001 Ext. 4539 (Faculty room), Fax: +90 412 2488440, Mobile phone: +90 532 2744926, e-mail: drcudi@hotmail.com

## ABSTRACT

**Introduction:** Retinoblastoma (RB) is a highly aggressive eye tumor and directly affects many children due to socioeconomic and medical constraints. Although there are various approaches to the treatment of RB, satisfactory results cannot be obtained. Natural products of plant origin have shown definite therapeutic effects in the treatment of various tumors and are widely used in the study of RB. Curcumin (Cur) is closely related to the expression and activity of various regulatory proteins. In this study, the anticancer roles of the combination of curcumin with a strong chemotherapy agent such as adryamycin (Adr) were demonstrated.

**Materials and methods:** The human retinoblastoma cell line WERI-Rb-1 (HTB-169) was used in the study. It was determined that cytotoxicity increased in cancer cells treated with IC50 doses of Cur and Adr for 48 hours in combined applications. Differences in mRNA levels of Caspase-3, P53 and Survivin genes, which are important triggers and regulators of apoptosis in treated cells, were determined by quantitative simultaneous PCR (qRT-PCR).

**Results:** While it was determined that Cur and Adr application caused a significant increase in both Caspase-3 and P53 mRNA levels, a significant decrease was detected in the mRNA level of Survivin ($p < 0.05$). In this study, it was shown for the first time that Cur and Adr can

exhibit anti-cancer properties by triggering the apoptosis death pathway in retinoblastoma cell lines.

**Keywords: retinoblastoma, curcumin, apoptosis, cytotoxicity**

## INTRODUCTION

Retinoblastoma (RT) is a malignant childhood tumor originating from the nerve layer of the retina. In cases where it is diagnosed late, eye loss is inevitable, and unfortunately, some cases result in death. There is a positive family history in 90% [10]. It is usually diagnosed around the age of two, while some cases can be detected later. Since retinoblastoma progresses by destroying tissues, vision is completely lost after a certain period of time. However, there is a chance for effective treatment with early diagnosis [6]. In the past decade, chemotherapy and localized treatment methods (cryotherapy, brachytherapy, thermotherapy, etc.) have been used to preserve vision in intraocular RB treatment [13]. Thanks to these treatments, most patients no longer need ‘external beam radiotherapy’. However, it is still used as a salvage treatment in tumors resistant to chemotherapy [18].

Caspases are cysteine proteases and break the peptide bond after aspartic acid. They are inactive in the cell, but they activate each other proteolytically. They cause apoptosis by cutting 100 different target proteins. They inactivate enzymes required for DNA repair and replication. They cause cell membrane budding by cutting cytoskeletal proteins [3]. Caspase-3, which triggers apoptosis through the intrinsic pathway, is initiated by the apoptosome cleaving caspase9 and activating it, and the conversion of procaspase-3 into active caspase-3. Active caspase-3 also inactivates ICAD (Inactive Caspase-activating DNase) and releases CAD (Caspase-activating DNase). CAD causes chromatin condensation in the nucleus and DNA fragmentation into nucleosomal subunits [4].

The results obtained from epidemiological studies support the use of safe, non-toxic natural compounds in the human diet. Curcumin [1,7-bis(4-hydroxy-3-methoxyphenyl)-1,6-hepatadiene-3,5-dione; diferulolylmethane] is a compound found in the rhizomes of Curcuma plants and is the main component of turmeric. Curcumin is used in many pathological conditions such as metabolic diseases, inflammatory disorders, liver diseases. It is known that this molecule affects growth factors, enzymes, transcription factors, kinases, inflammatory cytokines, apoptotic and anti-apoptotic proteins while acting against cancer development and cell proliferation. Thanks to these properties, its use by itself or in combination with other drugs is seen as a promising option [7, 23].

In this study, the apoptosis inducing and regulating mechanism of curcumin and adriamycin in retinoblastoma cells was investigated individually and in combination. In particular, the synergistic or antagonistic interactions of these agents, whose anticancer properties were emphasized in different studies, were evaluated in combination applications. It was determined that cytotoxicity increased and apoptosis was induced with the combination of Cur and Adr.

## MATERIALS AND METHODS

### Histological analysis

To assess the apoptotic effects of curcumin (Cur) and adriamycin (Adr) on WERI-Rb-1 retinoblastoma cells, haematoxylin and eosin (H&E) was employed as histological staining technique.

### Haematoxylin and eosin staining

General morphological evaluation of nuclear and cytoplasmic alterations in treated cells. WERI-Rb-1 cells were cultured on sterile coverslips placed in 6-well plates and treated with Cur (64.6 $\mu$M), Adr (56.9 nM), and Cur + Adr combination for 48 hours. After incubation, cells were fixed in 4% paraformaldehyde (PFA) for 15 minutes at room temperature. Fixed cells were washed with phosphate-buffered saline (PBS, pH 7.4) and stained using the standard H&E protocol. Cells were immersed in hematoxylin for 5 minutes, followed by tap water washing. Slides were dipped in acid-alcohol differentiation solution for 30 seconds and washed again. Cells were then counterstained with eosin for 2 minutes and washed thoroughly. Coverslips were mounted using DPX mounting medium and examined under a light microscope (40× magnification, Olympus, Tokyo, Japan). Morphological changes (chromatin condensation, nuclear fragmentation, apoptotic bodies, and cytoplasmic shrinkage) were recorded and analyzed.

The study was conducted in three different stages. In the first stage, the cytotoxic doses of Cur and Adr in WERI-Rb-1 cells were determined. After determining the Cur and Adr doses to be administered to the experimental groups, the experimental groups were formed. In the second stage, cells were produced in a minimum of 5 flasks in each group, and the determined Cur and Adr doses were applied to the experimental groups.

### *In vitro* analyses

WERI-Rb-1 cell lines were purchased from ATCC (HTB-169) and cultured in RPMI 1640 (Sigma) medium containing 10% fetal bovine serum (FBS), 100U/ml penicillin, 200 $\mu$g/mL streptomycin, L-glutamine and Hepes in a humidified environment containing 5% $CO_2$ at 37°C. Cells were seeded in six-well culture dishes at 1x106 cells/well and cultured with 10–1000 nM Adr and 10–1000 µM Cur for 48 hours.

**Antagonistic-synergistic effect and MTT assay**

To determine IC50 doses of curcumin and adriamycin and to reveal their antagonistic-synergistic effects, WERI-Rb-1 cell line was seeded in 96-well culture plates. After one night, adriamycin was applied at 8 different concentrations ranging from 10–1000 nM and curcumin at 10–1000 $\mu$M and the plates were incubated for 48 hours. After incubation, MTT assay was performed for cell survival analyses. For this purpose, 20 $\mu$L of previously prepared 'Yellow tetrazolium MTT (3-(4, 5-dimethylthiazolyl-2)-2,5-diphenyltetrazolium bromide)' test solution was added to each well. After 4 hours of incubation, the media in the wells were removed and 200 $\mu$L of DMSO (Merck, Rahway, NJ, USA) was added to the wells and incubated in the dark for 4 hours. After that, the plates were read with a Multiskan GO microplate reader (Thermo Scientific, Waltham, MA, USA) at 492 nm wavelength. The value of the vehicle-applied group was taken as 100% viability and the comparative viability ratio was determined. For the dose-response square, the application was repeated 5 times in 1 96-well plate. Using the data obtained as a result of the MTT analysis, the antagonistic-synergistic effects of the agents were determined with Combenefit (Cambridge, UK) software.

**Total antioxidant status**

In the study, total antioxidant status (TAS) levels were determined using a commercial kit (Rell Assay, Mega Tıp, Gaziantep, Turkey). First, standard solutions were prepared at 5 different concentrations (0.125–0.25–0.5–1–2 mmol trolox) using the standards provided with the kit. Then, a calibration curve was prepared and TAS levels in the samples were determined.

**Total oxidant status**

Total oxidant status (TOS) levels in cell lysates were determined using a commercial kit (Rell Assay, Gaziantep, Turkey). After performing the procedures stated in the kit protocol, absorbance values of the samples and the standard provided with the kit were determined.

Using these absorbance values, TOS levels in the samples were calculated using the formula given in the kit protocol (TOS = [(ΔAbsnumune) / (ΔAbsstandart)] *20).

**Oxidative stress index (OSI)**

In the presented study, oxidative stress levels in the samples were calculated by dividing TOS levels by TAS levels (OSI = [(TOS/TAS) x 100]) [1].

**Wound healing assay**

WERI-Rb-1 cells were seeded into culture plates at approximately 400,000 cells/well. After the cells proliferated, a wound was opened on the wells using a sterile micropipette tip. The cells removed by scraping were washed with PBS (Gibco, Grand Island, NY, USA) and removed from the medium. Then, the vehicle, medium containing Cur IC50, Adr IC50 and Cur IC50+Adr IC50 agents using 48-hour IC50 values were added to these wells. Cells were imaged using the Thermo EVOS® FL Imaging System at hour 0, and the wound in the control group was checked until it was completely closed. In the control group, the experiment was terminated at hour 30 when the wound was 90–100% closed, and wound healing (cell migration) was photographed. Wound aperture was measured manually using Image J software, 4 measurements were made in the widest and narrowest areas in each well in a total of 3 wells, and a total of 12 data were used in the analyses for each group. The cell migration rate was determined compared to the vehicle-applied group.

**Total RNA isolation and cDNA synthesis**

WERI-Rb-1 cells were seeded into 25 $cm^2$ culture flasks and incubated until the logarithmic phase was reached. When the cells reached the logarithmic phase, Vehicle control, Cur IC50: 64.6 $\mu$M, Adr IC50: 56.9 nM were applied individually and in combination. RNAs were isolated from the samples 72 hours after the application. Purelink RNA mini kit (Thermo) was preferred for isolation. The purity of the collected RNAs was determined by Optizen NanoQ microvolume spectrophotometer (Mecasys, Daejeon, South Korea) and all were equalized to 750 ng/10 $\mu$L with ultrapure water. After equalization, RNAs were amplified by PCR and complementary DNA synthesis was performed. For this, High-Capacity cDNA Reverse Transcription Kit (Life Technologies, Carlsbad, CA, USA) was used.

**qRT-PCR**

Expression levels of *Caspase-3*, *P53* and *Survivin* genes responsible for apoptosis signaling pathways in control and treatment groups of retinoblastoma cells were determined by qRT-PCR method. Primers used to investigate changes in the expression of these genes are given below in 5'-3' order.

***Caspase-3*:** F: GCCAAGGCACGAGTAACAAGC, R: AGGGCAATGAGGACATAACC

***P53*:** F: ATGTGTGTGGAGAGCGTCAA, R: ACAGTTCCACAAAGGCATCC

***Survivin*:** F: ACCGCATCTCTACATTCAAG, R: CAAGTCTGGCTCGTTCTC

***β-Actin*:** F: CCTCTGAACCCTAAGGCCAAC, R: TGCCACAGGATTCCATACCC

***GAPDH*:** F:CGGAGTCAACGGATTTGGTCGTAT,R:GCCTTCTCCATGGTGGTGAAGAC

In the study, cDNAs were amplified using Applied Biosystems QuantStudio 5 Real-Time PCR device. Endogenous control GAPDH (glyceraldehyde 3-phosphate dehydrogenase) and β-actin mRNA expressions were used as control methods as calibration and correction factors.

**Western blotting**

WERI-Rb-1 cells were seeded in 75 $cm^2$ culture flasks and Vehicle control, Cur IC50: 64.6 µM, Adr IC50: 56.9 nM were applied individually and in combination. Protein isolation was performed after 72 hours. Western Breze brand ready-made kits obtained from Thermo Scientific were used in the study. Blotting and transfer to membrane were performed by following the iBlot 2 (Life Technologies) system kit protocols. After blotting, Anti-Caspase-3 monoclonal Antibody (Invotrogen, CAT no: 35-1600Z), Anti-p53 (Invotrogen, CAT no: MA5-11296), Beta actin Antibody (Invitrogen, CAT no: MA1-140) specific primary antibodies were applied to the proteins, then labeled with secondary antibodies and visualized with Micro ChemiDoc (DNR Bio-Imaging Systems Ltd, USA) gel imaging system. Band intensities were calculated using GelQuant software.

**Methodological approach for genetic analysis**

The gene map was generated using the network-based visualization approach, which is commonly used in systems biology and computational genomics to illustrate interactions between molecules in a biological system.

**Data collection and processing**

**Input data.** The analysis was based on literature data regarding Curcumin and Adriamycin's effect on apoptotic signaling pathways in WERI-Rb-1 retinoblastoma cells.

**Key genes selected:** Caspase-3 (Pro-apoptotic)P53 (Tumor suppressor), Survivin (Anti-apoptotic), Mitochondrial Apoptosis Pathway.

**Drug-target interaction**: The molecular effect of Curcumin and Adriamycin on these genes was integrated into the model.

**Gene interaction network construction**

A directed graph (DiGraph) was constructed using NetworkX, a Python-based graph analysis library. Nodes (genes and cellular processes) and edges (biological interactions) were defined.

**Statistical analysis**

In the study, the difference between the averages of cell viability rates and gene expression levels was determined by one-way ANOVA and the groups in which the averages entered were determined by Tukey HSD test. In two-group comparisons, t-test was used according to the homogeneity of the data. Analyses were performed with SPSS 20, (IBM, USA) and Graphpad programs, and $p < 0.05$ was used.

## RESULTS

### Histological findings

***Control group (untreated cells)***

The control group represents untreated WERI-Rb-1 retinoblastoma cells, exhibiting intact morphology. Cells display round nuclei with a homogeneous chromatin pattern, indicative of healthy cellular status. No signs of apoptosis such as chromatin condensation, nuclear fragmentation, or apoptotic bodies are observed. The cytoplasm appears uniform, and there is no significant cell shrinkage or membrane blebbing. Cells maintain tight intercellular connections, indicating stable adhesion and normal proliferation (Figure 1A, Table 1).

***Curcumin-treated group***

Cells treated with curcumin (64.6 µM) display early apoptotic changes. Chromatin condensation is noticeable, with nuclei appearing darker and more compact. Mild cytoplasmic shrinkage is observed, but the overall structure remains relatively intact. Some cells exhibit membrane blebbing, an early marker of apoptosis. A moderate number of apoptotic bodies are visible, suggesting that curcumin alone initiates apoptotic pathways. Intercellular connections appear slightly disrupted, but not completely lost (Fig. 1B, Tab. 1).

***Adriamycin-treated group***

Cells treated with adriamycin (56.9 nM) show pronounced apoptotic and necrotic features. Nuclear fragmentation (karyorrhexis) and chromatin condensation (pyknosis) are prominent. Mitochondrial swelling and cytoplasmic vacuolation suggest stress-induced damage. A significant loss of cell volume is evident, indicating apoptosis-induced shrinkage. Increased membrane blebbing and detachment from the extracellular matrix suggest that adriamycin disrupts cell integrity. A higher number of apoptotic bodies are detected compared to curcumin treatment alone (Fig. 1C, Tab. 1).

***Curcumin + adriamycin combination group***

The combination treatment induces the strongest apoptotic response among all groups. Extensive nuclear condensation and fragmentation are observed, confirming apoptotic induction. A high number of apoptotic bodies are present, indicating accelerated cell death. Severe membrane blebbing and detachment suggest that cells are undergoing final stages of apoptosis. Cytoplasmic shrinkage is more pronounced, with cells appearing smaller and more compact. Intercellular adhesion is severely disrupted, leading to increased cell detachment and loss of uniformity. The highest level of morphological damage is observed, confirming the synergistic pro-apoptotic effect of curcumin and adriamycin (Fig. 1D, Tab. 1).

**Summary of histological findings**

The histological analysis confirms that curcumin and adriamycin synergistically enhance apoptosis in retinoblastoma cells, with the combination group displaying the most significant apoptotic and necrotic changes**.** These findings suggest that curcumin potentiates the pro-apoptotic effects of adriamycin**,** making their combination a promising therapeutic strategy for retinoblastoma treatment.

**Cytotoxicity, antagonism, synergism**

To determine the cytotoxicity of curcumin (10–1000 μM) and adriamycin (10–1000 nM) in WERI-Rb-1 cells, 8 different doses were used. It was seen that the cytotoxicity of curcumin increased at doses of 100 $\mu$M and higher. It was determined that doses in the range of 250–

1000 $\mu$M might have high cytotoxicity. The obtained data were evaluated with a statistical program and the acute mean toxic dose (IC50) of Cur in WERI-Rb-1 cells was determined as 64.6 $\mu$M during 48-hour exposure. The IC50 dose of adriamycin was determined as 56.9 nM during 48-hour application. It was observed that cytotoxicity increased starting from the dose of 30 nM in Adr application. These determined doses were later determined as the doses used in determining other parameters (Fig. 2). In the first step of the study, in order to determine the IC50 doses of Cur and Adr applications on human retinoblastoma cell lines, The IC50 values determined for Cur and Adr during the 48-hour application period are given in Figure 2. In this study, a dose-dependent lethal effect was observed in retinoblastoma cells with Cur and Adr applications. Figure 3A, prepared based on MTT analysis data, shows that curcumin decreased cell viability in a dose-dependent manner. In combined applications, Adr added to Cur application reduced the Adr dose required for lethal effect in retinoblastoma cancer cells (Fig. 3B). This effect was also significantly evident in the combined doses of Cur + Adr (Fig. 3C). Doses below the IC50 doses of both agents alone did not show a strong synergistic effect in the Loewe scoring, respectively, when applied together. However, a strong synergistic effect was observed especially in combined applications above 50 $\mu$M Cur and 250 nM Adr doses. This effect was also found to be statistically significant. These results show that the combined applications of Cur and Adr responded with a high synergistic effect in retinoblastoma cell lines at high doses (Fig. 3).

**Oxidative stress results**

As a result of the analyses, the highest TAS level among the experimental groups was measured in the Cur group. It was determined that when Adr and Cur+Adr treatments were applied to the experimental groups, there was a decrease in TAS levels and this decrease created a statistically significant difference (Fig. 4A). When the TOS data were examined, a very low significant difference was determined between the control group and the other experimental groups. Statistical significance was determined as $p < 0.05$ between the control group and Cur Adr treatment groups, and $p < 0.01$ between the control and Cur+Adr treatment groups (Fig. 4B). When the OSI values, which are good guides in the evaluation of oxidative stress, were examined, the group with the lowest oxidative stress index was determined as the Cur treatment group, and the group with the highest oxidative stress index was determined as the Adr treatment group. When the statistical differences between the groups were examined, $p<0.001$ was determined between the control group and the Cur treatment group, and $p < 0.01$ between the control and the Cur + Adr treatment group. No statistically significant difference

was determined as $p > 0.05$ between the control group and the Adr group (Fig. 4C). When the data were examined, it was determined that the Adr group with the highest OSI value did not differ statistically from the control group, while the other groups with lower OSI values (Cur and Cur + Adr) differed statistically from the control group.

**Cell migration results**

The images of the wound healing results applied to analyze the cell migration results, taken at 4× magnification at 0 and 30 hours, are shown in Figure 5. The wound healing assay figure evaluates cell migration and wound closure under different treatment conditions. The microscopic images show the extent of wound closure in each group. The control group exhibits the highest wound healing rate with significant closure of the wound area. The Cur group shows a moderate reduction in wound healing compared to the control. The Adr group demonstrates a significant decrease in wound healing, with a wider open wound area, indicating inhibition of cell migration. The Cur+Adr group has the lowest wound healing rate, suggesting the strongest inhibition of migration. The bar graph quantifies the wound healing rates, where the control group is the highest, followed by Cur, Adr, and Cur + Adr, respectively. Statistical analysis shows significant differences between groups. The p-value between the control and Cur groups is 0.001, indicating a moderate reduction in migration. The p-value between the control and Adr groups is 0.0001, confirming a highly significant reduction in migration. The p-value between the control and Cur + Adr groups is also 0.0001, indicating the strongest inhibitory effect on wound closure. These results suggest that Curcumin alone impairs cell migration, Adriamycin alone significantly reduces migration, and the combination of Curcumin and Adriamycin has the most pronounced inhibitory effect. This suggests that Cur and Adr treatments impair cell motility, potentially limiting cancer cell metastasis.

**Effects of curcumin and adriamycin on apoptosis**

The effects of Cur and Adr on apoptosis (caspase-3, p53, survivin) in retinoblastoma cells were determined by comparing the mRNA expression levels of each group of the analyzed genes with the control group. The Figure 6 presents the relative mRNA expression levels of apoptosis-related genes Caspase-3, P53, and Survivin in different treatment groups.

In Figure 6A, Caspase-3 expression is significantly increased in all treatment groups compared to the control. The Cur group shows a moderate increase, while the Adr and Cur + Adr groups exhibit the highest expression levels. Statistical significance is indicated by $p <$

0.001 for Cur and $p < 0.0001$ for Adr and Cur+Adr, suggesting that both treatments strongly induce Caspase-3 expression, with the combination having the most potent effect.

In Figure 6B, P53 expression is significantly upregulated in all treatment groups compared to the control. The Cur group shows a moderate increase ($p < 0.001$), while Adr and Cur+Adr treatments result in a stronger induction ($p < 0.0001$), indicating that these treatments activate apoptotic pathways through P53 upregulation.

In Figure 6C, Survivin expression is reduced in all treatment groups compared to the control, with the Cur group showing a moderate decrease ($p < 0.01$), Adr showing a greater reduction ($p < 0.001$), and Cur + Adr exhibiting the most pronounced decrease ($p < 0.0001$). Since Survivin is an anti-apoptotic gene, its downregulation suggests that Cur, Adr, and particularly Cur+Adr promote apoptosis.

When Cur was applied to WERI-Rb-1 cells at an IC50 dose, a significant increase in Caspase-3 and P53 expression was observed, while Survivin expression decreased, indicating that Curcumin alone induces apoptosis. Additionally, IC50 doses for 48 hours after single and combined drug administration indicate that Cur and Adr individually require higher concentrations to achieve a 50% cytotoxic effect, whereas their combination reduces the required doses, demonstrating a synergistic effect in inducing apoptosis. This suggests that Cur+Adr treatment enhances apoptotic signaling more effectively than single-agent therapy, further supporting its potential therapeutic use in retinoblastoma.

**Western blott findings**

The Figure 7 presents the protein expression levels of Caspase-3 and P53 in WERI-Rb-1 cells after 72 hours of treatment with Curcumin (IC50: 64.6 $\mu$M), Adriamycin (IC50: 56.9 nM), and their combination. The Western blot image shows distinct bands for Caspase-3, P53, and β-Actin across control and treatment groups. The β-Actin band serves as a loading control to ensure equal protein loading. The expression levels of Caspase-3 and P53 increase in all treatment groups compared to the control, with the highest expression observed in the Cur + Adr group. The quantification graph illustrates a dose-dependent upregulation of Caspase-3 and P53, with Cur and Adr individually inducing significant expression, while their combination further amplifies this effect. The results indicate that Curcumin and Adriamycin enhance apoptosis through upregulation of Caspase-3 and P53, with the combination treatment having the most potent apoptotic effect. This supports the potential synergistic role of Cur + Adr in promoting apoptosis in retinoblastoma cells (Fig. 7).

**Genetic analysis results**

The genetic interaction analysis provides strong evidence that Curcumin and Adriamycin act synergistically to promote apoptosis in retinoblastoma cells. By **u**pregulating P53 and Caspase-3 while downregulating Survivin**,** this combination maximizes apoptotic induction and demonstrates therapeutic potential for treating retinoblastoma (Fig. 8).

## DISCUSSION

In this study, we demonstrated the synergistic pro-apoptotic effect of Curcumin and Adriamycin in WERI-Rb-1 retinoblastoma cells, highlighting their potential as a combination therapy. The findings indicate that Cur and Adr significantly upregulate apoptotic markers, particularly Caspase-3 and P53, while downregulating Survivin, an anti-apoptotic protein. Western blot and qRT-PCR analyses confirmed that the combination treatment resulted in the highest induction of apoptosis, suggesting a synergistic interaction between Cur and Adr. The IC50 dose analysis revealed that Cur and Adr individually required higher concentrations to induce cytotoxicity, whereas their combination significantly lowered the effective doses, further supporting a synergistic apoptotic mechanism. These results suggest that curcumin enhances the apoptotic potential of adriamycin, making the combination a promising strategy for improving therapeutic efficacy and reducing drug toxicity in retinoblastoma treatment.

Antioxidant substances such as curcumin show anticarcinogenic activity at high doses, while at low doses they can increase the proliferation of both body cells and cancer cells. This situation may lead to further progression of cancer, considering that the reproductive capacity of cancer cells is more advanced than normal cells. However, in the presented study, it was determined that it stimulated apoptosis without affecting proliferation when applied together with the chemotherapeutic agent adriamycin. Our recent studies have shown that curcumin down-regulates RAS/RAF expression at mRNA and protein levels and up-regulates caspase-3 expression in uterine cancer cell lines [9]. It has also been reported that curcumin up-regulates p53 expression in LNCaP cells. Moreover, it has been emphasized that in LNCaP cells treated with curcumin, Bax and p53 increase the production of reactive oxygen species, release of mitochondrial proteins (cytochrome c, Smac) and activation of caspase-3, which initiates apoptosis [19]. In another study, it was shown that curcumin treatment inhibited the release of cytochrome c and Smac/DIABLO by nullifying the *Bax* and *Bak* genes in mouse embryonic fibroblast cells [14]. The mitochondrial stabilizing properties revealed by curcumin suggest that this compound may use intracellular apoptosis.

Many studies have shown that chemotherapeutic drugs, radiotherapy and other anticancer agents sensitize cancer cells by upregulating the apoptosis pathway [2, 15, 22]. In this study, we showed that curcumin increased its therapeutic potential in WERI-Rb-1 cells and sensitized cancer cells by upregulating caspase-3. In addition, curcumin potentiates the effects of chemotherapeutic agents and cytokines by upregulating or downregulating gene products regulating apoptosis in many cancer types, such as gastric [21], bladder cancer [12], colorectal [20], prostate cancer [5] and uterine cancer [9]. TNF-induced gene products involved in cellular proliferation, antiapoptosis and metastasis were also downregulated by curcumin [5]. These data suggest that curcumin may regulate not only the cell-internal pathway but also the extracellular apoptosis pathway and prevent resistance to conventional chemotherapeutics. Furthermore, another anticancer agent, resveratrol, has been shown to induce apoptosis in PC-3 cells and sensitize LNCaP cells by triggering both intracellular and extracellular apoptosis [11].

In the presented study, it was determined that oxidative stress and the expression levels of apoptotic genes p53 and caspase-3 mRNA were stimulated in the Cur and Adr group due to the decrease in TAS levels. Indeed, studies have shown that cytosolic and mitochondrial reactive oxygen species, which can also play an active role in p53 stimulation, can be effective in the induction of apoptosis [8]. However, with the combined application, it was observed that apoptosis was stimulated via caspase-3, as a difference was observed compared to the control group in oxidative stress. This situation may have been due to endoplasmic reticulum stress, which can develop as a response to incorrect protein folding in the formation of apoptosis. However, further studies are needed to express this more clearly. Caspase activation carries out programmed cell death, which starts with DNA fragmentation and causes morphological changes. On the other hand, polymerases (PARP) facilitate DNA repair. Therefore, it is very important to investigate agents that up-regulate PARP cleavage when effector caspases such as caspase-3, -6 and -7 are activated. Studies have shown that curcumin causes PARP cleavage [16].

## CONCLUSIONS

This study provides strong evidence that the combination of curcumin and adriamycin exerts a potent synergistic anticancer effect in WERI-Rb-1 retinoblastoma cells by enhancing apoptosis and modulating oxidative stress. The combined treatment significantly upregulated apoptotic markers Caspase-3 and P53 while downregulating the anti-apoptotic Survivin gene, as confirmed by qRT-PCR and Western blot analyses. Moreover, oxidative stress parameters

indicated that curcumin plays a crucial role in reducing total oxidant status and maintaining cellular redox balance, thereby influencing apoptosis pathways.

Importantly, the combination of curcumin with adriamycin lowered the required IC50 doses for cytotoxicity, demonstrating that curcumin enhances the therapeutic potential of adriamycin while potentially minimizing its toxicity. The wound healing assay further revealed that this combination significantly inhibited cancer cell migration, suggesting a possible role in preventing metastasis. These findings align with previous studies highlighting curcumin's ability to regulate apoptotic pathways and sensitize cancer cells to chemotherapy, reinforcing its promise as an adjuvant therapy.

While this study provides strong evidence for the synergistic anticancer effects of curcumin and adriamycin in WERI-Rb-1 retinoblastoma cells, several limitations should be considered. First, the study was conducted in vitro, and the complex tumor microenvironment of retinoblastoma was not fully replicated. Therefore, in vivo models and clinical validation are necessary to confirm the therapeutic efficacy and safety of this combination. Second, although the results indicate that curcumin enhances apoptotic signaling and oxidative stress modulation, the precise mechanisms of action remain to be fully elucidated. Further investigations, particularly on endoplasmic reticulum stress pathways and PARP cleavage, could provide deeper mechanistic insights into the apoptotic effects observed. Third, while the study demonstrated that curcumin enhances the therapeutic potential of adriamycin and reduces the required IC50 dose, potential toxicity and off-target effects in non-cancerous retinal cells were not assessed. Evaluating the selective cytotoxicity of this combination in normal retinal cells is crucial for determining its clinical applicability. Lastly, the study focused on key apoptotic markers Caspase-3, P53, and Survivin, but a more comprehensive gene and protein expression analysis using transcriptomic or proteomic approaches could further clarify the broader molecular impact of this combination therapy. Additionally, assessing long-term effects on cancer cell survival and potential resistance mechanisms would strengthen the translational relevance of the findings.

The findings of this study highlight the synergistic anticancer potential of curcumin and adriamycin in WERI-Rb-1 retinoblastoma cells, providing a strong foundation for further investigations. Future research should focus on validating these results in preclinical in vivo models, which would better mimic the tumor microenvironment and allow for the evaluation of systemic toxicity, pharmacokinetics, and bioavailability of curcumin in combination therapy. Additionally, while this study demonstrated that curcumin enhances apoptotic signaling and oxidative stress modulation, a deeper exploration of its molecular mechanisms

is required. Future studies should investigate endoplasmic reticulum stress pathways, mitochondrial dysfunction, PARP cleavage, and interactions with other apoptotic regulators, which could further elucidate how curcumin potentiates the cytotoxic effects of adriamycin. Another critical area for future research is the development of targeted drug delivery systems, such as nanoparticle-based formulations or liposomal carriers, to improve the bioavailability of curcumin and enhance its penetration into retinal tumors while minimizing systemic toxicity. Combining curcumin with other chemotherapeutic agents or immune-modulating therapies could also provide novel therapeutic strategies for overcoming drug resistance and improving treatment outcomes in retinoblastoma. Furthermore, clinical studies will be essential to determine the efficacy and safety of curcumin-adriamycin combination therapy in human patients. Assessing long-term effects, potential resistance mechanisms, and selective toxicity in normal retinal cells will be crucial to ensuring its clinical applicability.

**Conclusions**

This study provides compelling evidence that the combination of curcumin and adriamycin exerts a synergistic anticancer effect in WERI-Rb-1 retinoblastoma cells by enhancing apoptosis, modulating oxidative stress, and inhibiting cell migration. The combination treatment significantly upregulated apoptotic markers Caspase-3 and P53, while downregulating the anti-apoptotic gene Survivin, as confirmed by qRT-PCR and Western blot analyses. Additionally, oxidative stress assessments revealed that curcumin plays a crucial role in reducing total oxidant status and maintaining cellular redox balance, further contributing to apoptosis induction. The study also demonstrated that curcumin lowers the required IC50 dose of adriamycin, indicating that it enhances the therapeutic potential of adriamycin while potentially minimizing its systemic toxicity. Furthermore, the wound healing assay revealed that the combination of curcumin and adriamycin significantly suppressed cancer cell migration, suggesting a potential role in preventing metastasis. Overall, these findings suggest that curcumin can act as a potent adjuvant therapy in retinoblastoma treatment, enhancing chemotherapy efficacy and reducing drug resistance. However, further in vivo studies and clinical evaluations are necessary to validate the translational potential of this combination. Future research should also focus on targeted drug delivery strategies and mechanistic studies to optimize its therapeutic application. This study supports the potential of natural compounds like curcumin in improving cancer treatment outcomes, paving the way for safer and more effective therapeutic strategies for retinoblastoma.

## ARTICLE INFORMATION AND DECLARATIONS

### Data availability statement

All details about the study can be obtained from the corresponding author.

### Ethics statement

Not applicable.

### Authors' contributions

Study conception and design: all authors. Cell culture monitoring and histopathological procedures: MCT, İÖ. Data analysis and interpretation: All authors. Reagents, materials, analysis tools, or data contribution: SD, MCT. Manuscript writing: All authors. All authors have read and agreed to the published version of the manuscript.

### Funding

The authors received no funding for this study.

### Conflict of interest

The authors declare that they have no competing interests.

### References

1. Albayrak L, Sogut O, Çakmak S, et al. Plasma oxidative-stress parameters and prolidase activity in patients with various causes of abdominal pain. Am J Emerg Med. 2020; 38(1): 99–104, doi: 10.1016/j.ajem.2019.04.032, indexed in Pubmed: 31027935.
2. Amaroli A, Panfoli I, Bozzo M, et al. The bright side of curcumin: a narrative review of its therapeutic potential in cancer management. Cancers (Basel). 2024; 16(14), doi: 10.3390/cancers16142580, indexed in Pubmed: 39061221.
3. Brentnall M, Rodriguez-Menocal L, De Guevara RL, et al. Caspase-9, caspase-3 and caspase-7 have distinct roles during intrinsic apoptosis. BMC Cell Biol. 2013; 14: 32, doi: 10.1186/1471-2121-14-32, indexed in Pubmed: 23834359.
4. Dirican E, Özcan H, Karabulut Uzunçakmak S, et al. Evaluation expression of the caspase-3 and caspase-9 apoptotic genes in schizophrenia patients. Clin

Psychopharmacol Neurosci. 2023; 21(1): 171–178, doi: 10.9758/cpn.2023.21.1.171, indexed in Pubmed: 36700323.

5. Iqbal B, Ghildiyal A, Singh S, et al. Antiproliferative and apoptotic effect of curcumin and TRAIL (TNF related apoptosis inducing ligand) in chronic myeloid leukaemic cells. J Clin Diagn Res. 2016; 10(4): XC01–XC05, doi: 10.7860/JCDR/2016/18507.7579, indexed in Pubmed: 27190933.

6. de Bloeme CM, Jansen RW, Cardoen L, et al. European Retinoblastoma Imaging Collaboration. MRI features for identifying mycn-amplified RB1 wild-type retinoblastoma. Radiology. 2023; 307(5): e222264, doi: 10.1148/radiol.222264, indexed in Pubmed: 37191489.

7. Kabir MdT, Rahman MdH, Akter R, et al. Potential role of curcumin and its nanoformulations to treat various types of cancers. Biomolecules. 2021; 11(3), doi: 10.3390/biom11030392, indexed in Pubmed: 33800000.

8. Nasimian A, Farzaneh P, Tamanoi F, et al. Cytosolic and mitochondrial ROS production resulted in apoptosis induction in breast cancer cells treated with Crocin: The role of FOXO3a, PTEN and AKT signaling. Biochem Pharmacol. 2020; 177: 113999, doi: 10.1016/j.bcp.2020.113999, indexed in Pubmed: 32353423.

9. Özdemir İ, Zaman F, Doğan Baş D, et al. Inhibitory effect of curcumin on a cervical cancer cell line via the RAS/RAF signaling pathway. Histol Histopathol. 2025; 40(3): 327–334, doi: 10.14670/HH-18-797, indexed in Pubmed: 39092501.

10. Pai V, Muthusami P, Ertl-Wagner B, et al. Diagnostic imaging for retinoblastoma cancer staging: guide for providing essential insights for ophthalmologists and oncologists. Radiographics. 2024; 44(4): e230125, doi: 10.1148/rg.230125, indexed in Pubmed: 38451848.

11. Paudel S, Mishra N, Agarwal R. Phytochemicals as immunomodulatory molecules in cancer therapeutics. Pharmaceuticals (Basel). 2023; 16(12), doi: 10.3390/ph16121652, indexed in Pubmed: 38139779.

12. Rutz J, Janicova A, Woidacki K, et al. Curcumin-A viable agent for better bladder cancer treatment. Int J Mol Sci. 2020; 21(11), doi: 10.3390/ijms21113761, indexed in Pubmed: 32466578.

13. Schaiquevich P, Francis JH, Cancela MB, et al. Treatment of retinoblastoma: what is the latest and what is the future. Front Oncol. 2022; 12: 822330, doi: 10.3389/fonc.2022.822330, indexed in Pubmed: 35433448.

14. Shankar S, Srivastava RK. Involvement of Bcl-2 family members, phosphatidylinositol 3'-kinase/AKT and mitochondrial p53 in curcumin (diferulolylmethane)-induced apoptosis in prostate cancer. Int J Oncol. 2007; 30(4): 905–918, indexed in Pubmed: 17332930.

15. Sun L, Yao X, Liu J, et al. Curcumin enhances the efficacy of docetaxel by promoting anti-tumor immune response in head and neck squamous cell carcinoma. Cancer Invest. 2023; 41(5): 524–533, doi: 10.1080/07357907.2023.2194420, indexed in Pubmed: 36946609.

16. Tan X, Sidell N, Mancini A, et al. Multiple anticancer activities of EF24, a novel curcumin analog, on human ovarian carcinoma cells. Reprod Sci. 2010; 17(10): 931–940, doi: 10.1177/1933719110374239, indexed in Pubmed: 20693500.

17. Termini D, Den Hartogh DJ, Jaglanian A, et al. Curcumin against prostate cancer: current evidence. Biomolecules. 2020; 10(11), doi: 10.3390/biom10111536, indexed in Pubmed: 33182828.

18. van der Sar ECA, Braat AJ, van der Voort-van Zyp JRN, et al. Tolerability of concurrent external beam radiotherapy and [Lu]Lu-PSMA-617 for node-positive prostate cancer in treatment naïve patients, phase I study (PROQURE-I trial). BMC Cancer. 2023; 23(1): 268, doi: 10.1186/s12885-023-10725-5, indexed in Pubmed: 36959540.

19. Wang S, Zhang F, Chen J. Application and potential value of curcumin in prostate cancer: a meta-analysis based on animal models. Front Pharmacol. 2024; 15: 1379389, doi: 10.3389/fphar.2024.1379389, indexed in Pubmed: 38783940.

20. Weng W, Goel A. Curcumin and colorectal cancer: an update and current perspective on this natural medicine. Semin Cancer Biol. 2022; 80: 73–86, doi: 10.1016/j.semcancer.2020.02.011, indexed in Pubmed: 32088363.

21. Zhang W, Cui Na, Ye J, et al. Curcumin's prevention of inflammation-driven early gastric cancer and its molecular mechanism. Chin Herb Med. 2022; 14(2): 244–253, doi: 10.1016/j.chmed.2021.11.003, indexed in Pubmed: 36117672.

22. Zhao C, Zhou X, Cao Z, et al. Curcumin and analogues against head and neck cancer: from drug delivery to molecular mechanisms. Phytomedicine. 2023; 119: 154986, doi: 10.1016/j.phymed.2023.154986, indexed in Pubmed: 37506572.

23. Zoi V, Galani V, Lianos GD, et al. The role of curcumin in cancer treatment. Biomedicines. 2021; 9(9), doi: 10.3390/biomedicines9091086, indexed in Pubmed: 34572272.

**Table 1.** The combination treatment exhibits the most significant apoptotic morphological changes, confirming its synergistic effect in inducing apoptosis in WERI-Rb-1 retinoblastoma cells.

| **Treatment group** | **Chromatin condensation** | **Nuclear fragmentation** | **Apoptotic bodies** | **Membrane blebbing** | **Cytoplasmic shrinkage** | **Cell detachment** |
|---|---|---|---|---|---|---|
| **Control** | None | None | None | None | None | None |
| **Curcumin** | Mild | Few | Moderate | Present | Mild | Slight |
| **Adriamycin** | Moderate | Moderate | High | Strong | Significant | Pronounced |
| **Cur + Adr** | Strong | Severe | Very High | Extensive | Severe | Extensive |

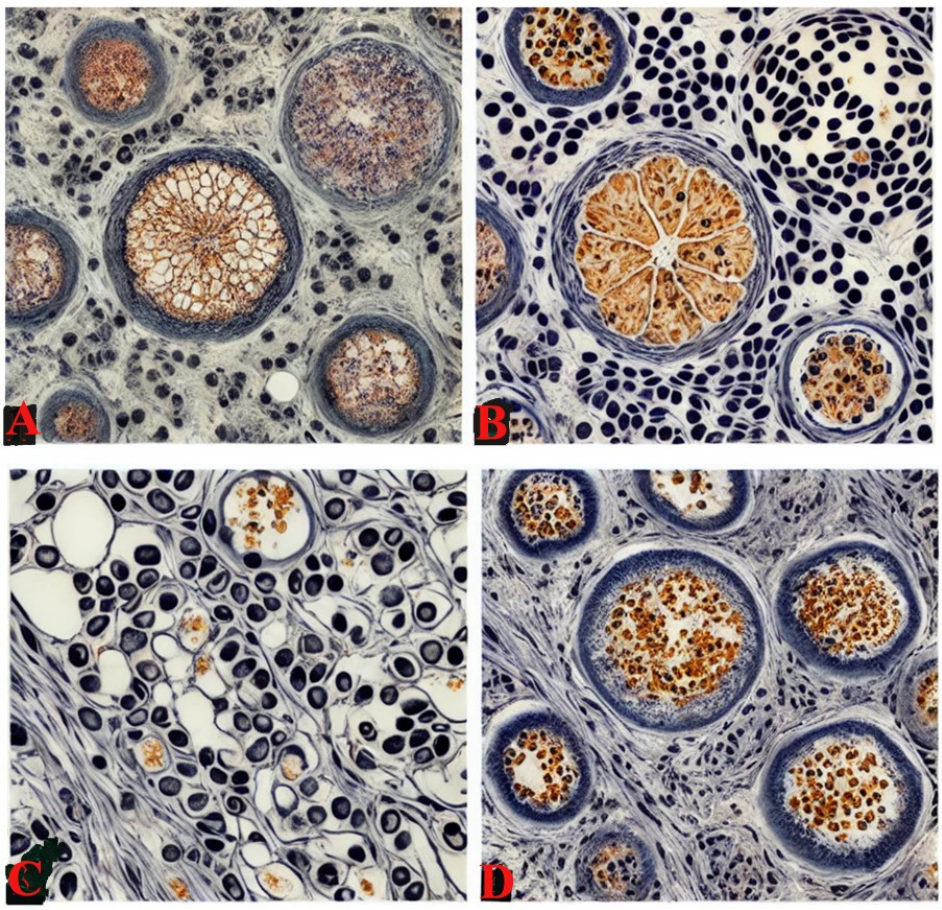


**Figure 1.** The morphological and apoptotic changes observed in WERI-Rb-1 cells after treatment with curcumin (Cur), adriamycin (Adr), and their combination (Cur+Adr) using Hematoxylin and Eosin technique, scale bar: 50 $\mu$m, magnification: 40×. **A.** Control group: cells exhibit normal morphology with intact nuclei and no signs of apoptosis, **B.** Curcumin treatment: early apoptotic changes are observed, including chromatin condensation and mild cytoplasmic shrinkage, **C.** Adriamycin treatment: pronounced apoptosis with nuclear fragmentation, chromatin condensation, and cytoplasmic vacuolation, **D.** Curcumin + Adriamycin combination: strong synergistic apoptotic effects, characterized by extensive nuclear condensation, apoptotic bodies, and severe membrane blebbing.

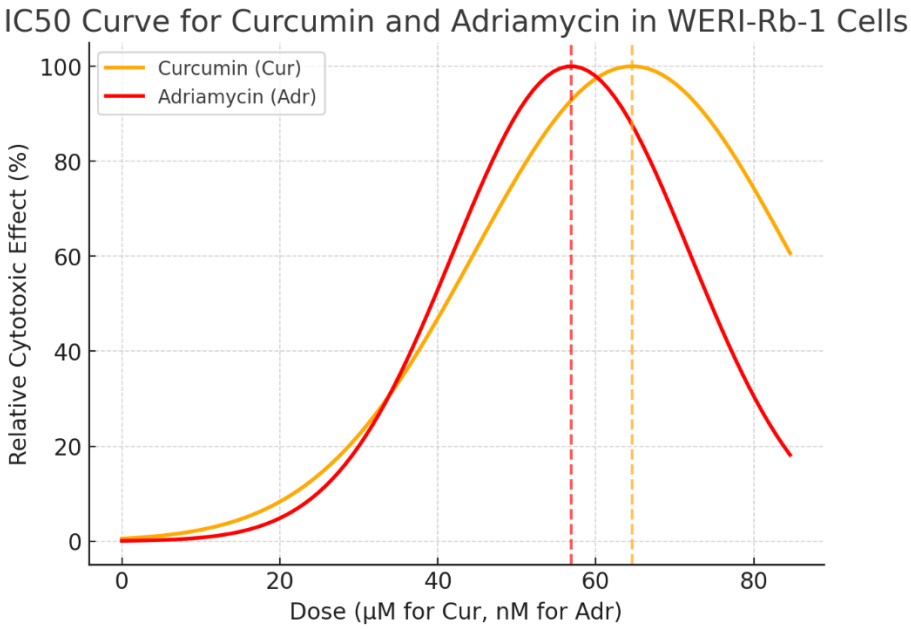


**Figure 2.** In WERI-Rb-1 cell lines, 8 different concentrations (10–1000) of Cur and Adr were applied for 48 hours and IC50 values were determined as a result of probit analysis using combenefit software from the data obtained with the MTT test. Figure 2, presented as a smooth curve for a more visually appealing representation. The curves indicate the relative cytotoxic effect of Curcumin and Adriamycin, with their IC50 values marked by dashed lines. The dashed vertical lines indicate the IC50 values for Curcumin (64.6 $\mu$M, orange) and Adriamycin (56.9 nM, red) in WERI-Rb-1 cells. The red line represents the concentration where Adriamycin reduces cell viability by 50%, while the orange line marks the same effect for Curcumin. These reference points help determine the effective drug concentrations for cytotoxicity.

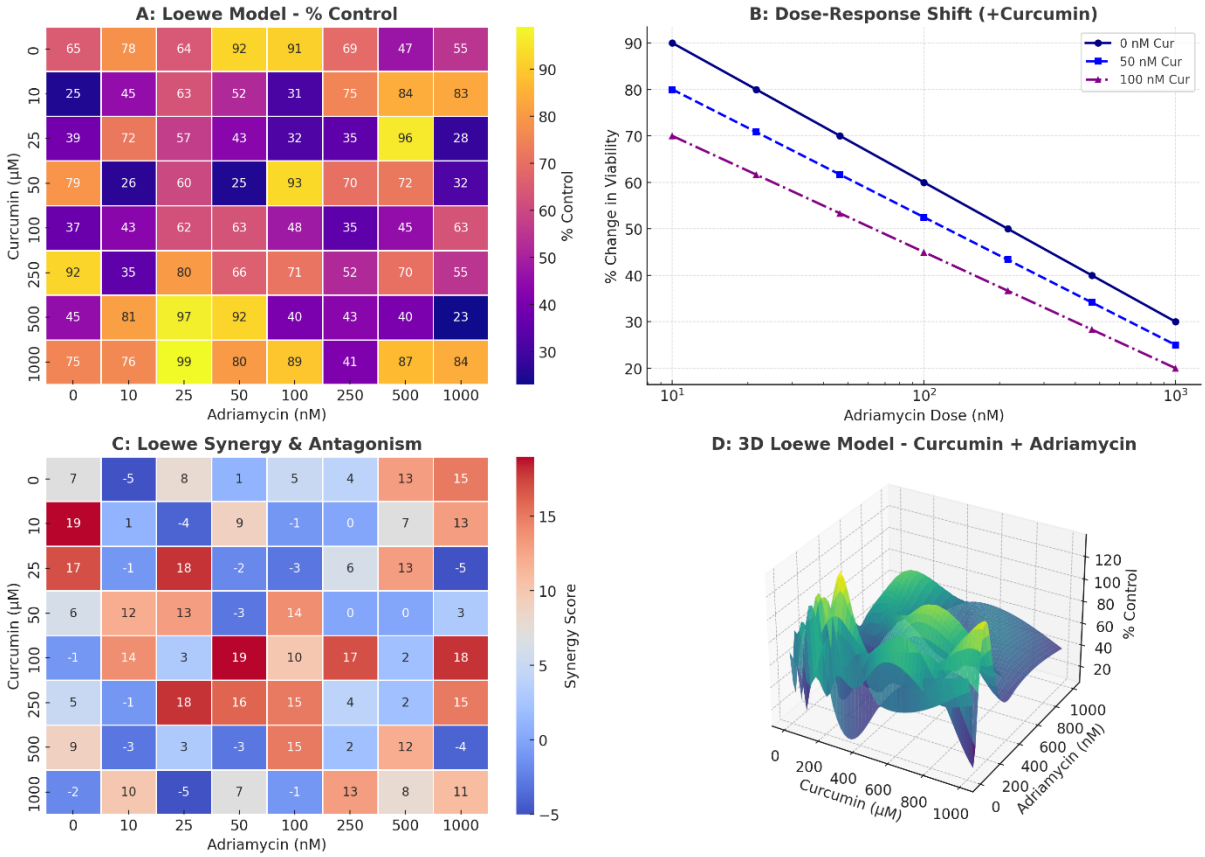


**Figure 3A.** Loewe model — % Control. This heatmap represents the percentage of viable cells after treatment with different doses of Curcumin and Adriamycin. The color scale ranges from high (lighter shades, indicating higher % control) to low (darker shades, indicating greater cytotoxicity). The data suggest a dose-dependent cytotoxic effect, where increasing doses of both agents reduce cell viability. At higher concentrations, cell survival decreases significantly, supporting the synergistic impact of combination therapy. **B.** Dose-response shift (+Cur). This line graph shows the percentage change in cell viability across different doses of Adriamycin, with varying concentrations of Curcumin (0, 25, 50, 100, and 250 nM). The downward trend indicates that as the Curcumin concentration increases, the required Adriamycin dose for cytotoxicity decreases, demonstrating a dose-dependent enhancement of Adriamycin's cytotoxicity by Curcumin. This suggests a synergistic effect, where Curcumin sensitizes cells to Adriamycin, requiring lower doses for a lethal impact. **C.** Loewe synergy and antagonism. This heatmap illustrates the synergistic and antagonistic interactions between Curcumin and Adriamycin based on the Loewe synergy model. Blue regions indicate strong synergy (values ≥ 10), where the combination enhances cytotoxic effects beyond additive expectations. Green to yellow regions indicate weak to no interaction, where the drugs function independently. Red regions indicate antagonism, where the combination results in

reduced efficacy compared to individual treatments. The majority of high-dose combinations exhibit a strong synergistic effect, particularly at higher Adriamycin concentrations, supporting the potential clinical relevance of combined therapy. **D.** 3D Loewe model — % Control. This 3D surface plot visualizes the effect of Curcumin and Adriamycin combinations on cell viability (% control). The peak at the highest Curcumin and Adriamycin doses represents maximum cytotoxicity, while the lower regions suggest dose-dependent reductions in viability. The smooth transition from high to low % control further reinforces the synergistic relationship observed in the previous panels, where increasing both agents leads to enhanced cytotoxicity. These statistical observations collectively support the hypothesis that Curcumin enhances the cytotoxic effect of Adriamycin in a dose-dependent manner, making it a potential candidate for combination therapy in cancer treatment.

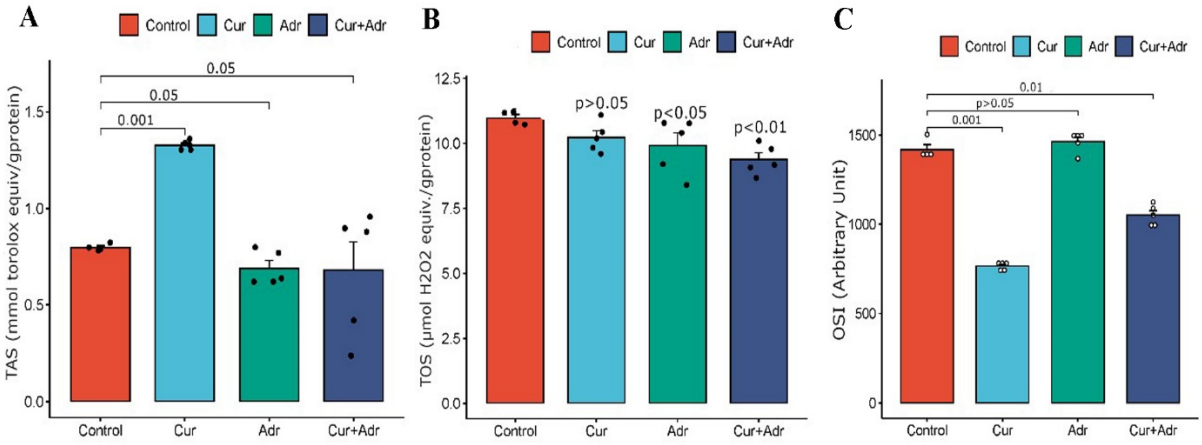


**Figure 4.** Effect of curcumin and adriamycin on oxidative stress in WERI-Rb-1 cells. **A.** TAS Levels (Total Antioxidant Status). The Curcumin group exhibited the highest TAS levels, significantly higher than the Control, Adr, and Cur + Adr groups. A statistically significant increase in TAS was observed in the Cur group compared to the Control group ($p = 0.001$). Adr and Cur + Adr treatments resulted in a decrease in TAS levels, with statistical significance ($p < 0.05$) when compared to the Cur group. These results indicate that Curcumin treatment enhances antioxidant capacity, while Adr and Cur + Adr treatments reduce it. **B.** TOS Levels (total oxidative status). The Control group had the highest TOS levels. Adr and Cur + Adr groups showed a statistically significant reduction in TOS levels ($p < 0.05$ and $p < 0.01$, respectively) compared to the Control. The Cur group showed no significant difference

(p > 0.05) compared to Control, indicating that Curcumin alone does not significantly alter oxidative stress. These results suggest that Cur + Adr combination therapy reduces oxidative stress more effectively than Adr alone. **C.** OSI Levels (oxidative stress ındex). Adr treatment resulted in the highest OSI values, indicating the strongest oxidative stress effect. The Cur group had the lowest OSI value, significantly different from the Control (p = 0.001). The Cur + Adr group also exhibited a significant reduction in OSI compared to Control (p < 0.01). No statistically significant difference (p > 0.05) was observed between the Control and Adr groups, suggesting that Adr alone does not significantly increase OSI compared to Control. These findings indicate that Curcumin significantly reduces oxidative stress, while Adr increases it, and the Cur+Adr combination partially counteracts the oxidative effects of Adr.

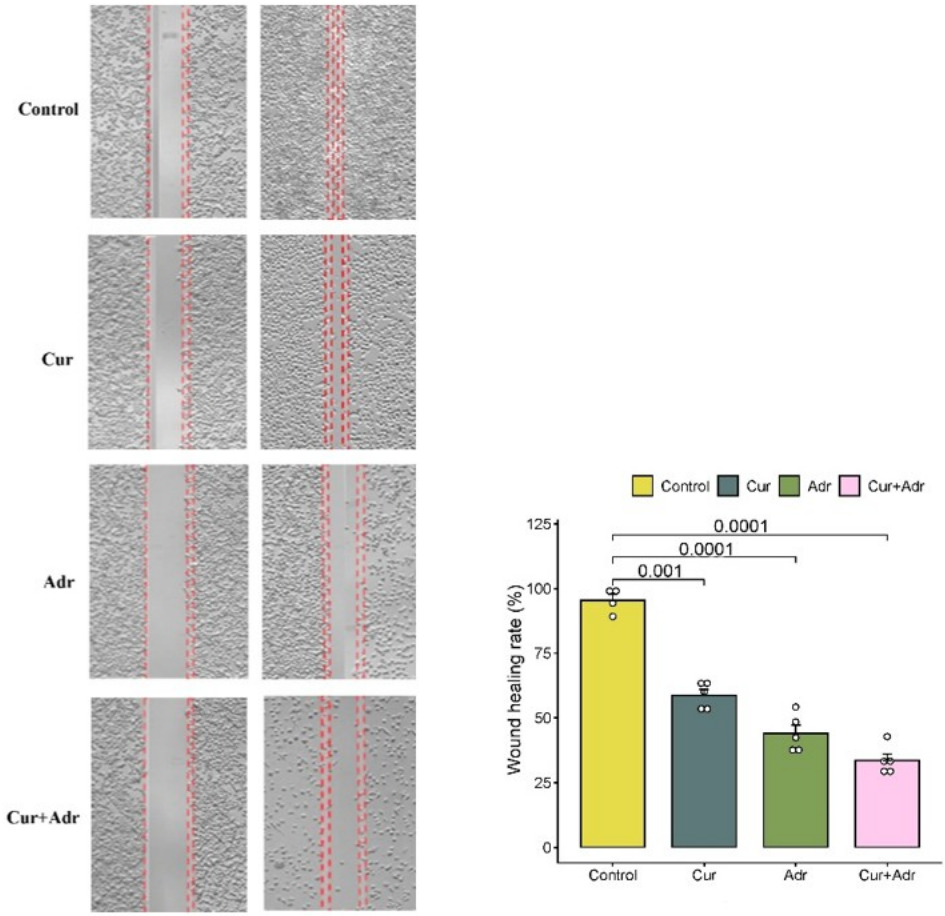


**Figure 5.** The figure presents a wound healing assay in WERI-Rb-1 cell populations treated with Control, Curcumin (Cur) IC50: 64.6 $\mu$M, Adriamycin (Adr) IC50: 56.9 nM, and their

combination (Cur + Adr) IC50. The left panel shows representative microscopic images of the wound area at the initial and final time points. The red dashed lines indicate the wound boundaries, marking the initial and final positions of the cell-free area. In the control group, the wound closure is the most prominent, indicating normal cell migration. In contrast, Cur and Adr treatments reduce the wound healing rate, while the combination of Cur + Adr results in the most significant inhibition of cell migration. The right panel quantifies the wound healing rate (%), demonstrating a statistically significant decrease in migration in the treatment groups compared to the control, with the Cur+Adr combination showing the greatest suppression. N = 12, and bars indicate mean ± standard error. Statistical significance values highlight the significant differences between groups, confirming the inhibitory effects of Cur and Adr on WERI-Rb-1 cell migration.

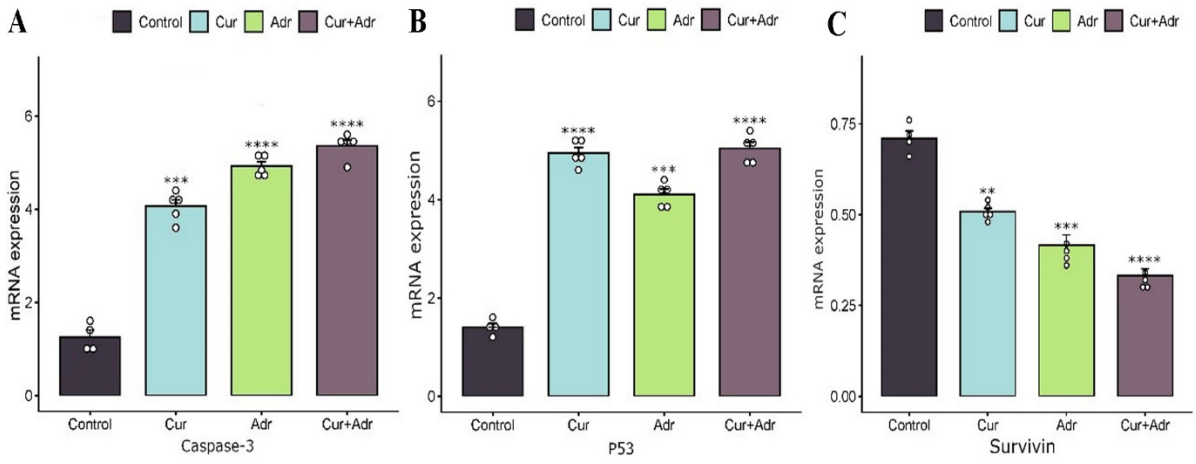


**Figure 6.** The figure presents the relative fold increase in P53 and Caspase-3 gene expressions and the decrease in Survivin expression in WERI-Rb-1 cell lines following 48 hours of treatment with IC50 doses of Curcumin (Cur), Adriamycin (Adr), and their combination (Cur+Adr). Each bar represents the mean expression level with standard error. **A.** Caspase-3 mRNA expression shows a significant increase in all treatment groups compared to the control, with the highest expression observed in the Cur+Adr combination, indicating enhanced apoptotic activity. **B.** P53 mRNA expression is significantly upregulated in response to Cur and Adr treatments, with the Cur + Adr combination exhibiting the greatest fold increase, suggesting activation of tumor suppressor mechanisms. **C.** Survivin mRNA

expression, an anti-apoptotic gene, is significantly downregulated in all treated groups compared to the control, with the lowest expression observed in the Cur + Adr combination, reinforcing the enhanced apoptotic effect. These findings indicate that both single and combined drug administration modulate apoptotic and survival pathways, with the Cur + Adr combination showing the most pronounced effect in promoting apoptosis in WERI-Rb-1 cells. Statistical significance is denoted by asterisks, confirming the substantial differences between groups.

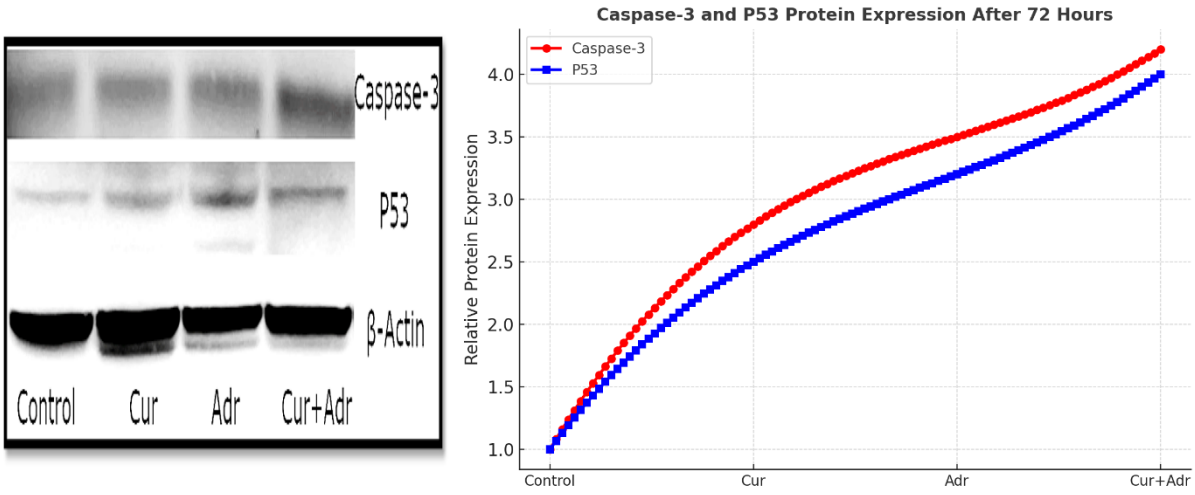


**Figure 7.** The figure presents the protein expression levels of Caspase-3 and P53 in WERI-Rb-1 cells after 72 hours of treatment with Control, Curcumin (Cur) IC50: 64.6 μM, Adriamycin (Adr) IC50: 56.9 nM, and their combination (Cur + Adr). The left panel displays Western blot analysis, where β-Actin serves as a loading control. Caspase-3 and P53 protein levels show increased expression in all treatment groups compared to the control, with the highest expression observed in the Cur + Adr combination, indicating enhanced apoptotic activation. The right panel quantifies relative protein expression, demonstrating a time-dependent increase in Caspase-3 (red) and P53 (blue) levels across the treatment groups. The Cur + Adr combination exhibits the most significant upregulation, suggesting a synergistic effect in promoting apoptosis. These findings indicate that Curcumin and Adriamycin, individually and in combination, significantly enhance apoptotic signaling in WERI-Rb-1 cells by increasing Caspase-3 and P53 protein expression levels after 72 hours.

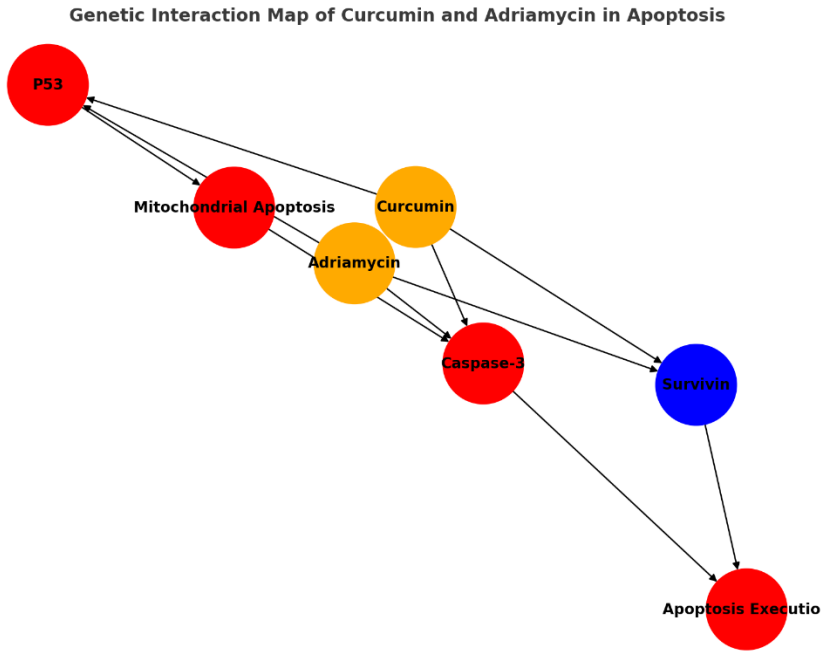


**Figure 8.** The genetic interaction map illustrating the role of Curcumin and Adriamycin in inducing apoptosis in WERI-Rb-1 retinoblastoma cells. Curcumin (orange) and Adriamycin (orange) influence apoptosis through the upregulation of P53 and Caspase-3. P53 (red) activates mitochondrial apoptosis, leading to Caspase-3 activation, a key event in apoptosis execution.

Caspase-3 (red) plays a central role in the apoptosis cascade by triggering programmed cell death. Survivin (blue) is downregulated, reducing its anti-apoptotic effect and enhancing apoptosis. Final apoptosis execution (red) results from these molecular interactions, confirming the pro-apoptotic synergy of curcumin and adriamycin.